Greener Synthesis of 1,2-Butylene Carbonate from CO_2 using Graphene-Inorganic Nanocomposite Catalyst

Victor Onyenkeadi[a], Suela Kellici[a] and Basudeb Saha[a*]

[a]Centre for Energy and Environment Research, School of Engineering, London South Bank University, 103 Borough Road, London SE1 0AA, UK.

[*] Corresponding Author: Centre for Energy and Environment Research, School of Engineering, London South Bank University, 103 Borough Road, London SE1 0AA, UK. T: +44 (0) 20 7815 7190; F: +44 (0) 20 7815 7699; E-mail: b.saha@lsbu.ac.uk.

List of Figures

List of Tables

Abstract[†]

The synthesis of 1,2-butylene carbonate (BC) from cycloaddition reaction of 1,2-butylene oxide (BO) and carbon dioxide (CO_2) was investigated using several heterogeneous catalysts in the absence of organic solvent. Continuous hydrothermal flow synthesis (CHFS) has been employed as a rapid and cleaner route for the synthesis of a highly efficient graphene-inorganic heterogeneous catalyst, ceria-lanthana-zirconia/graphene nanocomposite, represented as Ce–La–Zr/GO. The heterogeneous catalysts have been characterised using transmission electron microscopy (TEM), X-ray photoelectron spectroscopy (XPS), X-ray powder diffraction (XRD) and nitrogen adsorption/desorption (BET for measuring the surface area/pore size distribution),. Ceria- lanthana-zirconia/graphene nanocomposite catalyst (Ce–La–Zr/GO) exhibited high catalytic activity as compared to other reported heterogeneous catalysts in the absence of any organic solvent with a selectivity of 76% and 64% yield of 1,2-butylene carbonate at the reaction conditions of 408 K, 75 bar in 20 h.

Keywords: 1,2-butylene carbonate (BC), carbon dioxide (CO_2), continuous hydrothermal flow synthesis (CHFS), ceria, lanthana and zirconia graphene oxide nanocomposite (Ce-La-Zr/GO), heterogeneous catalysts.

[†] Abbreviations : BC, 1,2-butylene carbonate; BO, 1,2-butylene oxide; CO_2, Carbon dioxide;CHFS, Continuous hydrothermal flow synthesis; Ce-LA-Zr/GO, Ceria lanthana, and zirconia graphene oxide; Ce-La-Zr-O, Ceria and lanthana doped zirconia; BET, Brunauer–Emmett–Teller; SEM, scanning electron microscope; TEM, Transmission electron microscopy; XRD, x-ray diffraction; (XPS), X-ray photoelectron spectroscopy; Ce-Zr-O, Ceria doped zirconia; (EC), ethylene carbonate; (CMEC), (chloromethyl) ethylene carbonate; (VCHC), 4-vinyl-1-cyclohexene carbonate; (MgO), magnesium oxide; (GO), graphene oxide; FID, Flame ionization detector; GC, Gas chromatograph; La-O, Lanthanum oxide; (La-ZrO_2), Lanthana doped zirconia; (ZrO_2), Zirconium oxide; (CeO_2), Cerium oxide; MEL Chemicals, Magnesium Elektron Limited Chemicals; PO, propylene oxide; PC, propylene carbonate; t, time (h); scCO2, Supercritical CO2; SCF, Supercritical fluid, (NGP), Natural graphite powder; (HCL), Hydrochloric acid; (H_2SO_4), Sulphuric acid; (K_2O_2), sodium nitrate, potassium hydroxide pellet; (H_2O_2), Hydrogen peroxide; (C_3H_6O), Acetone; (C_8H_{18}), Octane; ($KMnO_4$), Potassium permanganate; (CH3OH), Methanol; ($Ce(NO_3)_3 \cdot 6H_2O$), Cerium(III) nitrate hexahydrate; ($La(NO_3)_3{\cdot}6H_2O$), Lanthanum (III) nitrate hexahydrate; (ZrO(NO3)2 · xH2O), Zirconium (IV) oxynitrate hydrate.

1. INTRODUCTION

The global emission of carbon dioxide (CO_2) into the atmosphere has reached unsustainable level resulting in climate change and therefore there is the need to reduce the emission of CO_2 [1]. Recently, there has been a tremendous interest in the use of CO_2 as an environmentally benign building block in the chemical industry due to its chemical and physical properties (e.g. chemical inertness, stability, non-flammability, non-toxicity) allowing to be considered as an attractive green replacement of toxic reactants (e.g. isocyanates, phosgene) [2,3]. CO_2 is regarded as a stable compound due to its carbon covalently bonded to two oxygen atoms, although the thermodynamic stability of CO_2 requires a significant amount of energy to be decomposed [4]. There are known ways in which CO_2 emissions could be reduced such as replacing fossil fuels with renewable energy [5], carbon capture and storage (CCS) [6] and CO_2 utilisation [7]. The use of CO_2 for the synthesis of valuable products such as cyclic carbonates and polycarbonates *via* greener routes is highly desirable. The reactions of CO_2 with epoxides are exothermic and generate organic carbonates such as cyclic [8] and polycyclic carbonates [9].

Organic carbonates such as acyclic, cyclic and polycyclic carbonates are widely used chemicals in agriculture, automobile, cosmetic, lithium battery, paint and pharmaceutical industries [10,11]. Cyclic carbonates such as ethylene carbonate (EC), 1,2-butylene carbonate (BC), propylene carbonate, (PC), (chloromethyl) ethylene carbonate (CMEC), 4-vinyl-1-cyclohexene carbonate (VCHC) and styrene carbonate (SC) have been synthesised through the direct synthesis of CO_2 with their respective epoxides in the presence of either homogeneous or heterogeneous catalysts, but only a few have been commercialised [12,13].

1,2-butylene carbonate is a valuable chemical of great commercial interest. It is an excellent reactive intermediate material used in industry for the production of plasticisers, surfactant, and polymers and can also be used as a solvent for degreasing, paint remover, wood binder resins, foundry sand binders, lubricants as well as a potential solvent for lithium battery as energy generation because of its high polarity property [14,15]. The significance of this research is not only to reduce CO_2 emission in the atmosphere, which causes global warming, but also to produce a value-added chemical.

There have been several routes reported for the synthesis of cyclic carbonates that include the followings: oxidative carboxylation of alkenes [15], oxidative carbonylation of alcohol and

phenol [17], the reaction of urea and phenol or alcohol, phosgene and oxetanes [18], and direct synthesis of CO_2 with epoxides [19].

These processes of cyclic carbonates synthesis use toxic materials and produce harmful by-products, which are cancer-causing substances. These toxic materials could pose a severe health challenge and a threat to the environment. The shortcomings of the traditional approach remains a major challenge in recent times.

Recent studies have shown that the use of catalysts has not only facilitated the process of greener organic carbonates synthesis but enhanced the selectivity of the desired products and fulfilled the requirement for the sustainability of the greener chemical process [11].

Various homogeneous catalytic processes have been studied extensively such as ionic liquid [20], salen metal complex [21], salt and metal halide [22], for the synthesis of cyclic carbonate through the catalytic reaction of CO_2 and epoxides. However, the processes have suffered various drawbacks due to the high cost of catalyst production, difficulty in separation of product from the reaction mixture, complexity of processes, co-solvent use, potential production of toxic species, limitation of catalyst reusability and instability of the catalyst under room condition [23,24].

Several metal oxide catalysts have been developed and assessed for the effective synthesis of cyclic carbonates such as magnesium oxide (MgO) [25], graphene oxide (GO) [26], zirconium oxide (ZrO_2) [27], cerium oxide (CeO_2) [27], lanthanum oxide (La_2O_3) and a mixed metal oxide such as ceria doped zirconia oxide (Ce-ZrO_2) [28], Furthermore, it has been identified that the use of support can enhance the dispersion of the active sites, the stability of catalyst, and consequently offer improvements of the catalytic properties of the material. Recent studies have shown numerous materials have been used extensively as suitable supports such as activated carbon, silica, molecular sieves, metal oxides and graphene oxide [29].

Graphene (a unique 2D single layer of one atom thick sp2 carbon) and its derivatives represent an advanced class of catalysts materials with novel characteristics (very high surface area and easy surface modifications) [30–32]. Indeed, in this paper, we report the use of graphene derivative (ceria-lanthana-zirconia/graphene nanocomposite) as high-quality catalyst material (highly stable and active) prepared via controlled, easily scalable continuous hydrothermal flow synthesis (CHFS).

The use of CHFS reactors over conventional means gives an independent control over reaction variables such as temperature, flow rate and pressure [33]. The process of CHFS involves the continuous mixing of supercritical water stream with an aqueous precursor/flow (typically

metal salts) to produce spontaneous precipitation of nanoparticles with desirable composition and properties.

The catalytic activities of the CHFS synthesised Ce-La-Zr/GO inorganic nanocomposite have been tested using a new, greener and sustainable process for the direct synthesis of 1,2-butylene carbonate from CO_2 with 1,2-butylene oxide. The effect of various parameters such as catalysis loading, reaction temperature, reaction time, CO_2 pressure has been studied. Catalyst reusability studies have been carried out to investigate the stability and reusability of the catalyst for the synthesis of BC.

2. EXPERIMENTAL

2.1. Materials

Table 1 lists the chemicals used and their respective sources. These chemicals were used without further pre-treatment or purification.

Table 1: List of chemicals and their sources

Chemicals	Chemical formula	Sources
Natural graphite powder (NGP)		Fisher Scientific UK Ltd
Hydrochloric acid	HCl	Fisher Scientific UK Ltd
Sulphuric acid	H_2SO_4	Fisher Scientific UK Ltd
Sodium nitrate	$NaNO_3$	Fisher Scientific UK Ltd
Potassium hydroxide pellet	KOH	Fisher Scientific UK Ltd
Hydrogen peroxide	H_2O_2	Fisher Scientific UK Ltd
Acetone	C_3H_6O	Fisher Scientific UK Ltd
Octane	C_8H_{18}	Fisher Scientific UK Ltd
Potassium permanganate	$KMnO_4$	Fisher Scientific UK Ltd
Methanol	CH_3OH	Sigma–Aldrich Co. LLC, UK
Cerium(III) nitrate hexahydrate	$Ce(NO_3)_3 \cdot 6H_2O$	Sigma–Aldrich Co. LLC, UK
Lanthanum (III) nitrate hexahydrate	$La(NO_3)_3 \cdot 6H_2O$	Sigma–Aldrich Co. LLC, UK
Zirconium (IV) oxynitrate hydrate	$ZrO(NO_3)_2 \cdot xH_2O$	Sigma–Aldrich Co. LLC, UK
1,2-butylene oxide	C_4H_8O	Sigma–Aldrich Co. LLC, UK
1,2-butylene carbonate	$C_5H_8O_3$	Sigma–Aldrich Co. LLC, UK
Magnesium oxide	MgO	Sigma–Aldrich Co. LLC, UK
Zirconium oxide and ceria,	ZrO_2	MEL Chemical Company Ltd

Cerium oxide	CeO_2	MEL Chemical Company Ltd
Lanthana oxide	La_2O_3	MEL Chemical Company Ltd
Lanthana doped zirconia	La-ZrO_2	MEL Chemical Company Ltd
Lithium doped zirconia	Li-ZrO_2	MEL Chemical Company Ltd
Ceria doped zirconia	Ce-ZrO_2	MEL Chemical Company Ltd
Lanthana doped zirconia	Ce-La-ZrO_2	MEL Chemical Company Ltd
Liquid carbon dioxide cylinder (99.9%)	CO_2	BOC Ltd., UK. All

2.2 Preparation and characterisation of ceria-lanthana-zirconia oxide/graphene nanocomposite synthesis via CHFS

2.2.1 Graphene Oxide (GO) Preparation

An improved method of Hummers and Offeman [34] was used to prepare GO from NGP using $KMnO_4$ as an oxidizing agent. 1.25 g of $NaNO_3$ and 1.25 g of NGP was added into 57.5 mL of H_2SO_4, which was stirred continuously with a magnetic stirrer in an ice bath for 15 mins. 10 g of $KMnO_4$ was added to the black slurry mixture gradually under a continuous stirring which was left for 15 mins. The resulting dark green mixture was transferred to an oil bath at 40 ^oC and stirred at 600 rpm for 90 mins. The deionised water of 100 mL was added slowly to the dark green mixture for about 15 mins then 15 mL of hydrogen peroxide (H_2O_2) was added in a dropwise manner for about 5 mins followed by another 100 mL of deionised water. The resulting light brown mixture was kept at 90 ^oC and stirred continuously at 600 rpm for 15 mins. The mixture was cooled to room temperature and the product was subject to centrifugation (5000 rpm, 5 mins per cycle). The product was washed with diluted HCl (10 mL of HCl in 80 mL deionised water) four times and deionised water three times in order to remove impurities. The GO was freeze-dried for 24 hrs.

2.2.2 Preparation of ceria-lanthana-zirconia oxide/graphene nanocomposite synthesis *via* CHFS

CHFS experiment was conducted using a reactor with a basic design that has been reported earlier [35-36]. CHFS simplified schematic of which is shown in Figure 1, mainly consists of three HPLC pumps (utilised for delivery of the water and desired precursors), counter-current reactor, cooler and back-pressure regulator. In a typical experiment, each pre-mixed aqueous

solution of $Ce(NO_3)_3.6H_2O$, $La(NO_3)_3.6H_2O$ and $ZrO(NO_3).6H_2O$ (with a total metal ion concentration of 0.2 M) Ce:La:Zr nominal atomic ratios (15:5:80) and pre-sonicated aqueous solution of GO (4 µgm/L) were pumped (*via* Pump 2) to meet a flow of KOH (1 M, delivered *via* Pump 3) at a T-junction (see Figure 1). The molar ratio of metal salt mixture $Ce^{3+}/La^{3+}/Zr^{4+}$ to GO was 1:1. This mixture meets superheated water (delivered *via* Pump 1 through the heater) at 24.1 MPa of 450 ^oC inside an in-house built countercurrent reactor whereupon the formation of Ce-La-Zr/GO occurred continuously [38,]. The aqueous suspension was cooled through a vertical cooler and slurries were collected from the exit of the back-pressure regulator (BPR). The product was separated *via* centrifugation (5000 rpm), washed with de-ionised water twice and then freeze-dried.

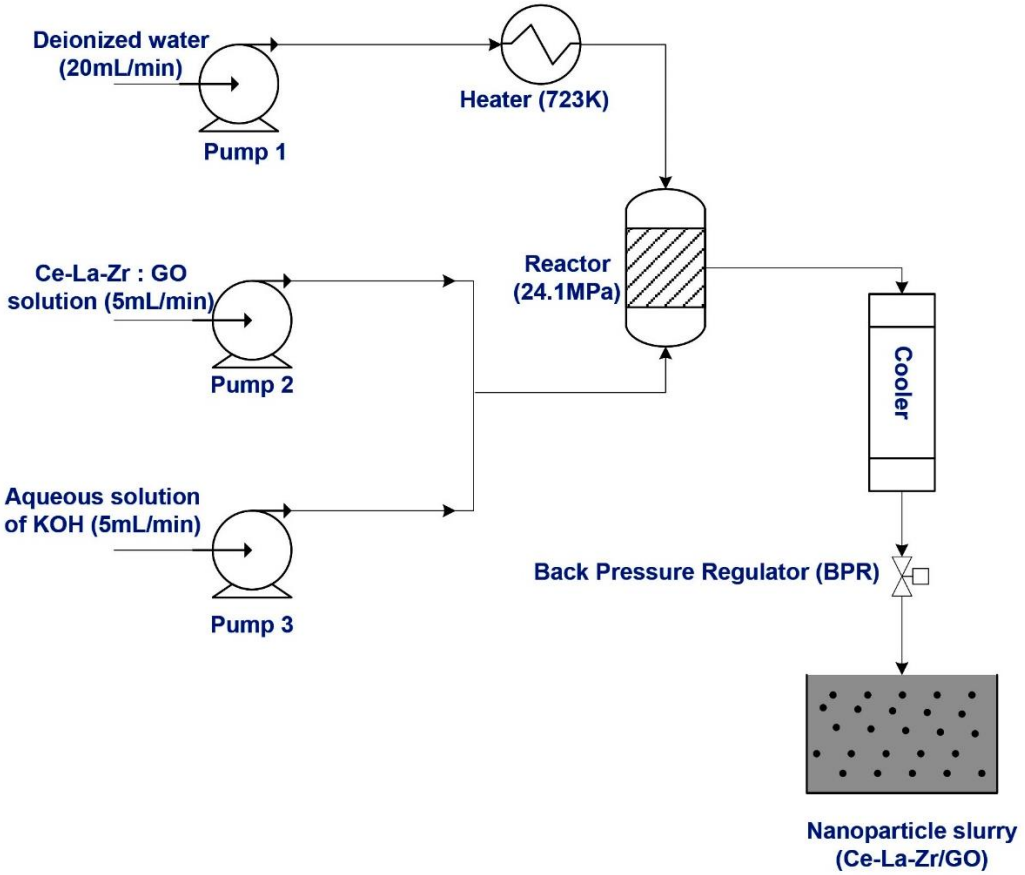

Figure 1: Schematic of a CHFS reactor set up used for the production of Ce-La-Zr/GO inorganic nanocomposite catalyst

2.3 Experimental procedure for the synthesis of 1, 2-butylene carbonate

The synthesis of BC was carried out in a 25 mL stainless steel high-pressure autoclave details of which have been reported previously [15] equipped with a stirrer, thermocouple and a heating mantle and controller. The reactor was charged with a required amount of BO and catalyst. The reactor was heated to the required temperature and continuously stirred at a known

stirring speed. The supercritical fluid pump was used to pump CO_2 at a desired pressure from the cylinder to the reactor and left for a specified time. The time at which the liquid CO_2 was charged into the reactor was taken as the starting time (t=0). After the reaction, the reactor was cooled down to room temperature using an ice bath.

The reactor was depressurized and the reaction mixture was filtered. The recovered catalyst was washed with acetone and dried in an oven while the products were analysed using a gas chromatography (GC) equipped with a flame ionization detector (FID) with a capillary column using octane as an internal standard. The effect of various parameters such as catalyst types, catalyst loading, CO_2 pressure, reaction temperature and reaction time was studied for the optimization of the reaction conditions. Catalyst reusability studies were also conducted to assess the stability of the catalyst for synthesis of BC.

2.4 Method of analysis

The separation and identification of experimental samples were done by Shimadzu gas chromatography (GC). The GC was equipped with a capillary column of dimension (30m x 320µm x 0.25 µm) and flame ionization detector (FID) as the detector. High purity (99.9%) helium was used as carrier gas at a flow rate of 1 mL/min. The injection and detector temperatures were maintained isothermally at 553 K. A split ratio of 50:1 and injection volume of 0.5 µL were chosen as a part of the GC method. A ramp method was used to differentiate all the components present in the sample mixture and the initial temperature was set at 323 K. An autoinjector was used to inject sample for analysis. The oven's temperature was set at 323 K for 5 min after the sample injection which was then ramped to 553 K at the rate of 25 K/min. The total run time for each sample was ~ 14min. After each run, the oven's temperature was cooled down to 323 K for successive sample runs. Octane was used as an internal standard. A chromatograph of sample mixture analysed using GC revealed that octane, BO and BC peak occurred at residence times of ~ 4, ~7 and ~12 respectively.

2.5 Equipment and catalyst characterisation techniques

Heto PowerDry PL3000 freeze-dryer has been used for freeze-drying all the samples. This was done by using liquid nitrogen to freeze the washed catalysts and left in a freeze drier for ca. 24 h.-TEM of Ce-La-Zr/GO was investigated using a JEOL 2100FCs with a Schotty Field Emission Gum transmission electron microscope (200 kV accelerating voltage). The sample was collected on the carbon-coated copper grid (Holey Carbon Film, 300 mesh Cu, Agar Scientific Essex, UK) after being briefly dispersed ultrasonically in water. BET surface area

measurements of heterogeneous catalysts were performed on a Micromeritics Gemini VII analyser (nitrogen adsorption and desorption method). Barrett-Joyner-Halenda (BJH) method was used to obtain the pore size distribution and pore volume. The XRD data of the prepared Ce-La-Zr/GO *via* CHFS reactor was collected on a Stoe Stadip diffractometer using Mo radiation (0.7093) angstrom wavelength) set at 30 mA, 50 kV using a Germanium 111 monochromatic crystal to select K alpha 1. A small amount of Ce-La-Zr/GO was placed between two polymer sheets clamped into a 3mm aperture holder and rotated in the X-ray beam. Dectris Mythen 1 K silicon strip Position Sensitive Detector (PSD) was used as a detector. Data were collected by scanning at position 2 to 45 2θ degree at 0.5^{o} steps and 30 seconds per step, the step resolution of the data being 0.015^{o}. LaB_6 standard was used to check diffractometer alignment.

XPS measurements were performed using a Kratos Axis Ultra DLD photoelectron spectrometer utilizing monochromatic Alka source operating at 144W. Samples were mounted using conductive carbon tape. Survey and narrow scans were performed at constant pass energies of 160 and 40 eV, respectively. The base pressure of the system is ca. 4×10^{-9} Torr under the analysis of these samples.

3. Results and discussion

3.1 Proposed reaction mechanism

The active acidic and basic site on the surface of mixed metal oxide catalyst plays a vital role in the synthesis of a cyclic carbonate and influences the selectivity of the product massively [47]. The reaction pathway for the synthesis of BC from the reaction of BO and CO_2 in the presence of the heterogeneous catalyst is shown in Figure 2a. The proposed reaction mechanism in which the metal atom M consists of Lewis acid site and an oxygen atom O consists of Lewis basic site is shown in Figure 2b. The reaction was initiated by adsorption of CO_2 on the basic site of the metal oxide catalyst to form a carboxylate anion and BO was activated by adsorption on the acidic site. The previous report has also suggested the parallel requirement of both Lewis base activation of the CO_2 and Lewis acid activation of the epoxide [48]. The carbon atom of BO is attacked by a carboxylate anion that leads to the ring opening of BO to form an oxyanion species and this was also supported by Adeleye et al [19]. BC formed as a product through desorption from the dissociation of metal oxide (catalyst) from the oxyanion species leads to a ring closure [27]. The side products associated with the reaction

of BO and CO_2 includes an isomer of BO and oligomers of BC which were below the detection limit of the GC-FID used in the analysis.

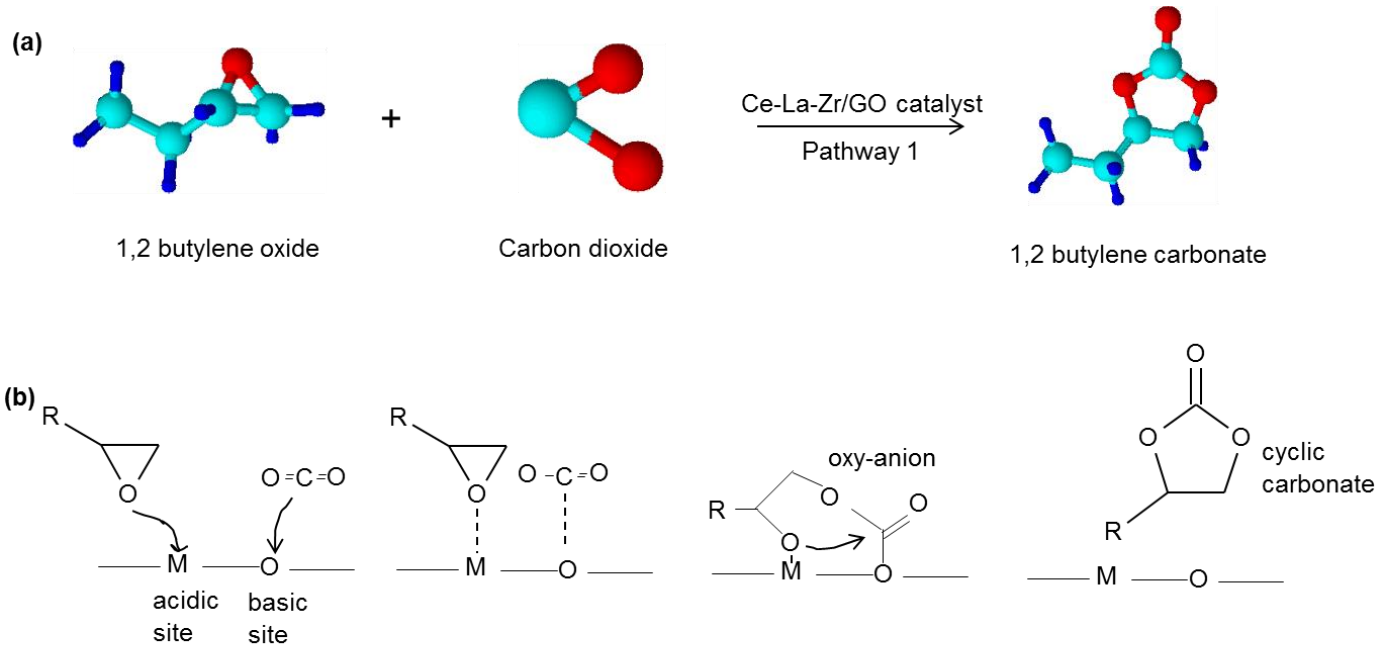

Figure 2: Synthesis of 1,2-butylene carbonate (BC) using a heterogeneous catalyst.

(a) Reaction scheme and (b) Plausible reaction mechanism.

3.2 Catalyst characterisation

In this work, rapid, single step, Continuous Hydrothermal Flow Synthesis (CHFS) approach was used for the synthesis of nanocomposite inorganic. Fig 3 shows a schematic representation of the synthesized Ce-La-Zr/GO inorganic nanocomposite. The Ce-La-Zr/GO inorganic nanocomposite was produced from 0.2 M (total concentration) of a pre-mixed aqueous solution of cerium, lanthanum and zirconium nitrate (Ce^{3+}: La^{3+}: Zr^{4+} at 15: 5: 80 atomic ratios) and GO (synthesised via conventional Hummer method) under alkaline conditions (KOH, 1M).

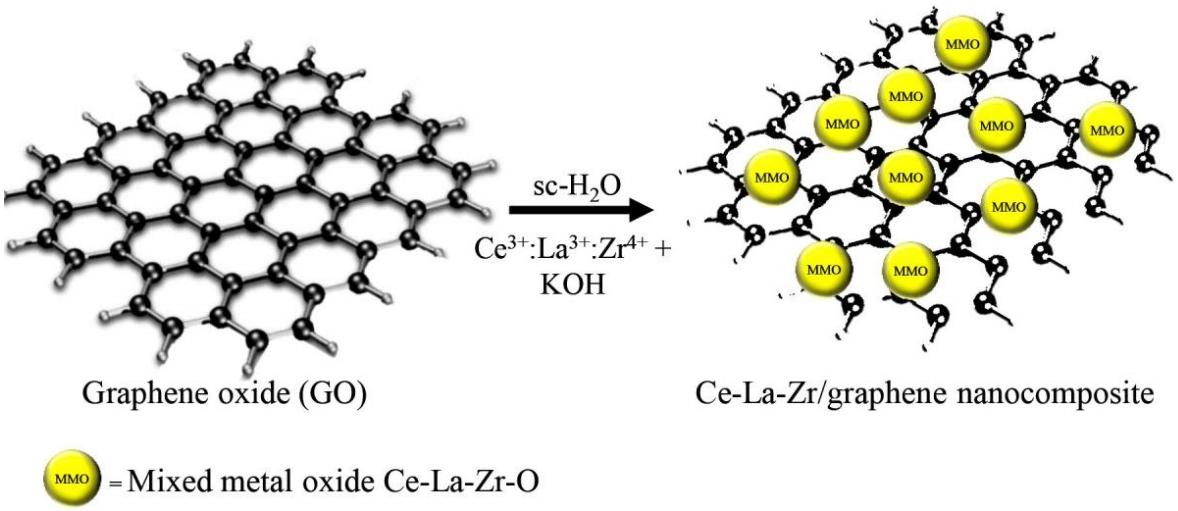

Figure 3: A schematic representation of the synthesized Ce-La-Zr/GO nanocomposite.

The transmission electron microscopy (TEM) images of GO and Ce-La-Zr/GO nanocomposite catalyst are shown in Figure 4, where Ce-La-Zr/GO catalyst exhibits a mean particle size of 5.78 ± 1.56 (see Table 2). Additionally, for comparative purposes, commercially available catalysts were also used for preliminary work and some of their characteristics are shown in Table 2.

X-ray powder diffraction (XRD) shown in Figure 5 was employed to assess the phase composition and crystallinity of CHFS as-prepared catalysts Ce-La-Zr/GO and GO (starting precursor). The XRD pattern of the nanocomposite matched with $Zr_{0.84}Ce_{0.16}O_2$ (ICDD standard card No. 38-1437) structure as indicated in the previously reported research [15].. The composition, oxidation states and chemical states of the as-synthesised materials wereexamined and analysed by X-ray photoelectron spectroscopy (XPS). Figure 6 shows the XPS analysis of the metal ratio of Ce-La-Zr/GO and the spin-orbit splitting of the La3d5/2 peak (ca. 4.5eV) indicating La_2O_3 phase for the latter. The spectra of samples revealed strong peaks corresponding to cerium, lanthanum, zirconium, oxygen and carbon. The hydrothermal process is effective in reducing GO as reported in by Kellici et al [42]. The C(1s) XPS spectra of Ce-La-Zr/GO made hydrothermally revealed the reduction of the peak intensities of the oxygen-containing functional group (epoxide, carboxyl and hydroxyl), which is associated with GO as starting material. The XPS analysis further revealed the presence of mixed Ce(III) and Ce (IV) species as evidenced by the peak at ca. 900 eV [43]. The XPS spectrum of the state Zr 3d core level shows a strong spin-orbit doublet due to ZrO_2 at 182.2 eV while at state 183.4 eV is due to Zr-OH bonds. The Zr-OH is supported by large O(1s) component at 531.4 eV[50]. The presence of suboxides is eliminated at these lower binding energies (ca 179-181 eV).

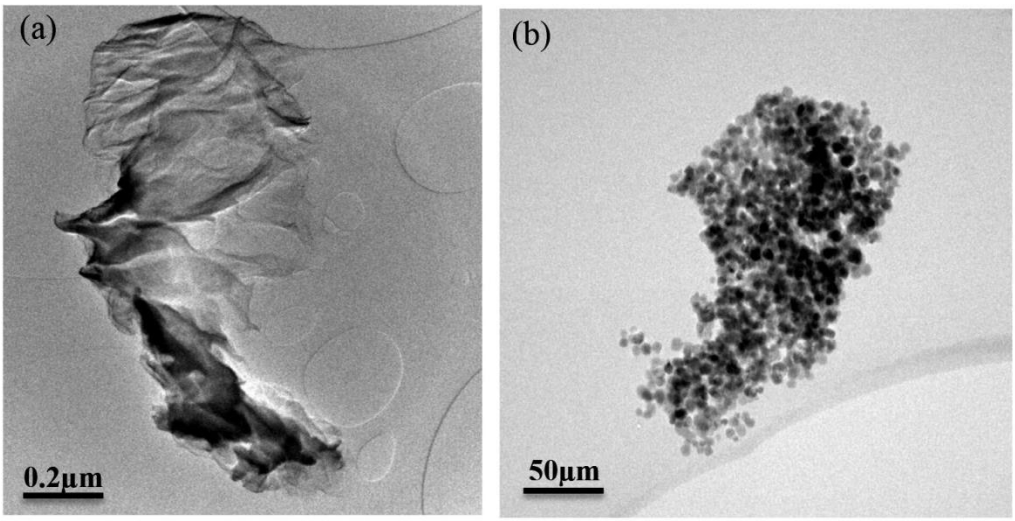

Figure 4: Transmission electron microscopy (TEM) images of (a) graphene oxide and (b) ceria, lanthana and zirconia graphene oxide (Ce-La-Zr/GO).

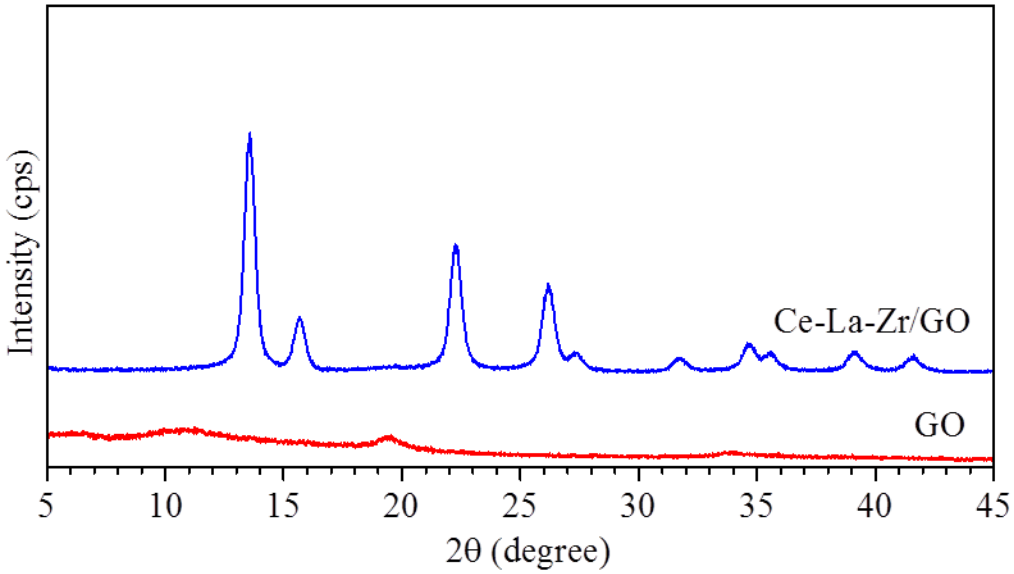

Figure 5: X-ray diffraction (XRD) patterns of ceria-lanthana - zirconia/graphene oxide (Ce-La-Zr/GO), and graphene oxide (GO) catalysts.

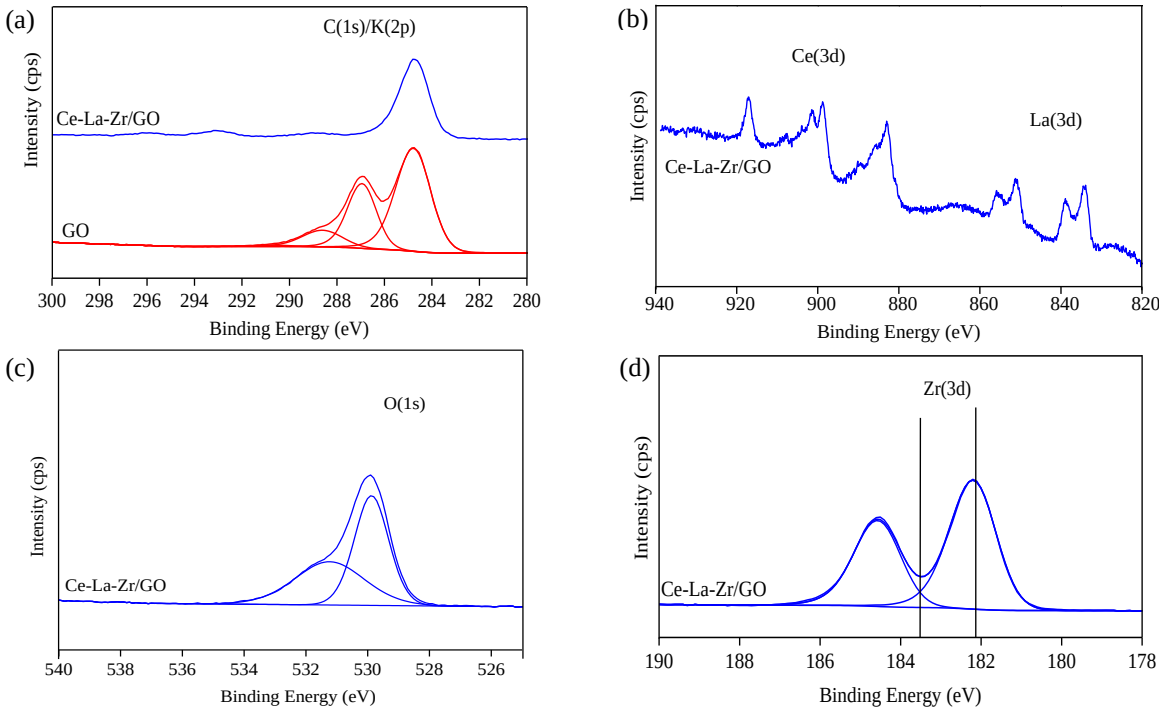

Figure 6: X-ray photoelectron spectroscopy (XPS) spectra showing (a) deconvoluted C(1s) (b) Ce(3d) and La(3d) region (c) O(1s) region and (d) Zr(3d) region for CHFS synthesized Ce-La-Zr/GO catalysts.

Table 2: Physical and Chemical Properties of Heterogeneous Catalysts and Synthesized Ce-La-Zr/GO Inorganic Nanocomposite Catalyst

Catalyst Properties	**Catalyst**						
	Zr-O	**GO**	**La-O**	**La-Zr-O**	**Ce-Zr-O**	**Ce-La-Zr-O**	**Ce-La-Zr/GO**
Physical form	White powder	Black powder	White powder	White powder	Pale yellow powder	Pale yellow powder	Black powder
Composition (%)	ZrO_2: 95±5	O: 24.64 C: 75.36	La_2O_3: 100	La_2O_3: 10±1 ZrO_2: 90±1	CeO_2: 18±2 ZrO_2: 82±2	CeO_2: 17±2 La_2O_3: 5±1 ZrO_2: 78±3	Ce: 2.98 La:1.19 O: 34.99 C: 47.29 K: 0.8 Zr: 12.75
BET surface area ($m^2\ g^{-1}$)	310	124	22	75	70	55	115
Pore volume ($cm^3\ g^{-1}$)	0.45	0.049	0.015	0.22	0.2	0.29	0.047
Particle size	5µm	-	100nm	5µm	30µm	1.7µm	5.78±3.9nm
Material synthesis Temperature (K)[a]	673 [a]	723 [b]	2578 [a]	673 [a]	673 [a]	673 [a]	723 [b]

[a]Manufacturer data and [b]CHFS data

3.3 Effect of mass transfer in heterogeneous catalytic reactions

In a heterogeneous catalytic reaction, the effect of mass transfer is very significant due to the reactants being indifferent phase from the solid catalyst unlike the homogeneous catalytic reaction, (where the reactant, catalyst, and yield are in the same phase), thereby making the effect of mass transfer between phases nearly negligible. Mass transfer plays a vital role in the reaction rate, the conversion of reactant and formation of product (yield) [44].The activity of a solid catalyst towards the selectivity of the desired product depends on the characteristics of the catalyst that includes (active site, molecular structure, pore size, porosity, surface area and particle size) and prevailing conditions at the boundaries of a solid catalyst such as (pressure, temperature, and superficial velocity).

The understanding of the effect of mass transfer in cycloaddition of CO_2 to BO in the presence of heterogeneous catalytic reaction offers a better understanding toward designing a new catalyst based on the limiting resistance for both internal and external mass transfer on the variable reaction parameters. Mass transfer of the reactants occurs from the bulk fluid to the external surface of the catalyst and diffuses from the external surface through the pores within the catalyst to the catalytic surface of the pores, in which the reaction occurs [45,46]. However, the external mass transfer resistance could be limited through the control of various parameters such as pressure, temperature and stirring speed. Furthermore, the understanding of catalytic reactions could limit the effect of mass transfer process during a chemical reaction and thereby shift the equilibrium towards the selectivity of the desired product.

The synthesis of BC through cycloaddition of CO_2 to BO was carried out using different stirring speed of 300 - 500 rpm. The results in Figure 7 shows that the conversion of BO and yield of BC were found to be the approximately same as there were no significant changes in the conversion and yield. The conversion of BO and yield of BC were found to be 84% and 64%, respectively with an experimental error of $\pm$2%. This confirmed that the external mass transfer resistance is negligible for the stirring speed from 300 rpm to 500 rpm under the related reaction conditions. Furthermore, the influence of internal mass transfer resistance is also negligible, and this is attributed to the size of the catalyst of 5-26 nm range, the average pore diameter of Ce-La-Zr/GO nanocomposite catalyst which was 2.16 nm and falls in the mesoporous region i.e. 2–50 nm reported by Clerici and Kholdeeva [47]. Moreover, the absence of internal and external mass transfer resistance using different stirrer speed and different size fractions of ion-exchange resins as catalysts for the synthesis of *n*-hexyl acetate has been reported by Patel and Saha [48]. The stirring speed of 300 rpm has been selected and used to conduct further

investigation for cycloaddition of CO_2 to BO for the synthesis of BC was as a result of energy efficiency and cost. Therefore, it can be concluded that there was no effect of mass transfer resistances on the synthesis of BC using Ce-La-Zr/GO catalyst at 300 rpm.

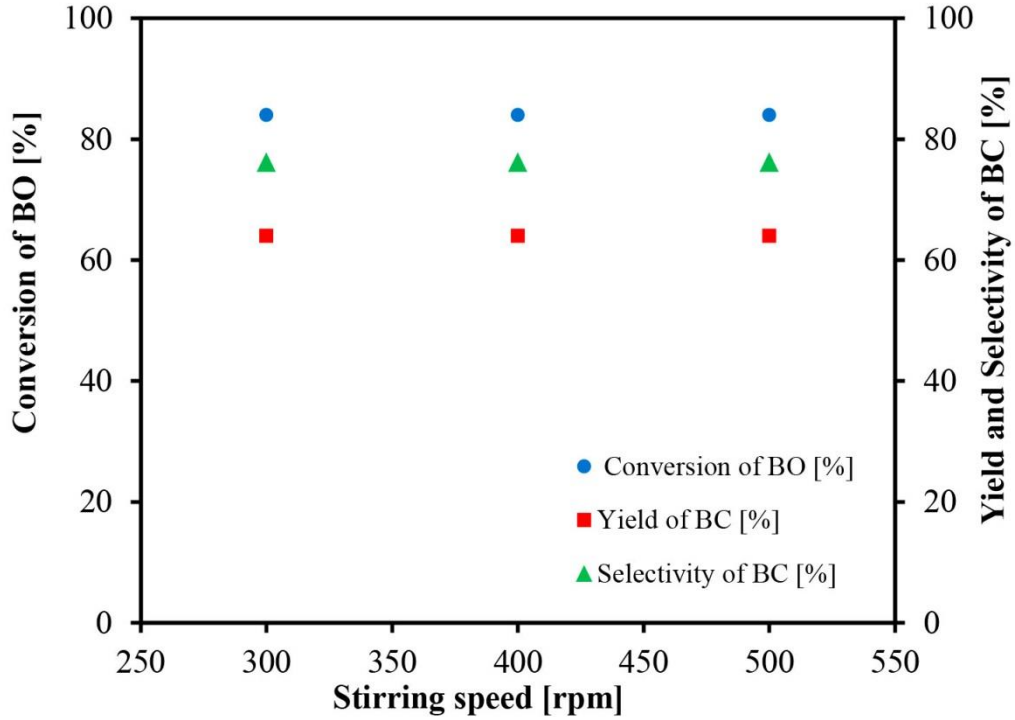

Figure 7: Effect of mass transfer resistance on conversion of 1, 2 butylene oxide (BO) against yield and selectivity of 1,2-butylene carbonate (BC). Experimental conditions: Catalyst - Ce-La-Zr/GO; Catalyst loading - 10% (w/w); CO_2 pressure - 75 bar; Reaction temperature - 408 K; Reaction time - 20 h.

3.4 Effect of different heterogeneous catalysts

The study of various heterogeneous catalysts such as catalytic activity, conversion, yield and selectivity were conducted in order to establish the best performing metal oxide or mixed metal oxide catalyst for the synthesis of BC through the cycloaddition reaction of CO_2 to BO using a high-pressure reactor. Figure 8 shows the results of different (commercially available) heterogeneous catalysts as well as Ce-La-Zr/GO (synthesised *via* CHFS) on the conversion of 1,2-butylene oxide, the yield and selectivity of 1,2-butylene carbonate. The experiments were conducted using the optimum reaction conditions. Ce-La-Zr/GO catalyst gave an improved conversion of BO (84%) and highest BC yield (64%) and selectivity (76%) at optimum reaction conditions of reaction temperature 408 K, CO_2 pressure 75 bar, reaction time 20 h, stirring speed 300 rpm and catalyst loading of 10% (w/w).

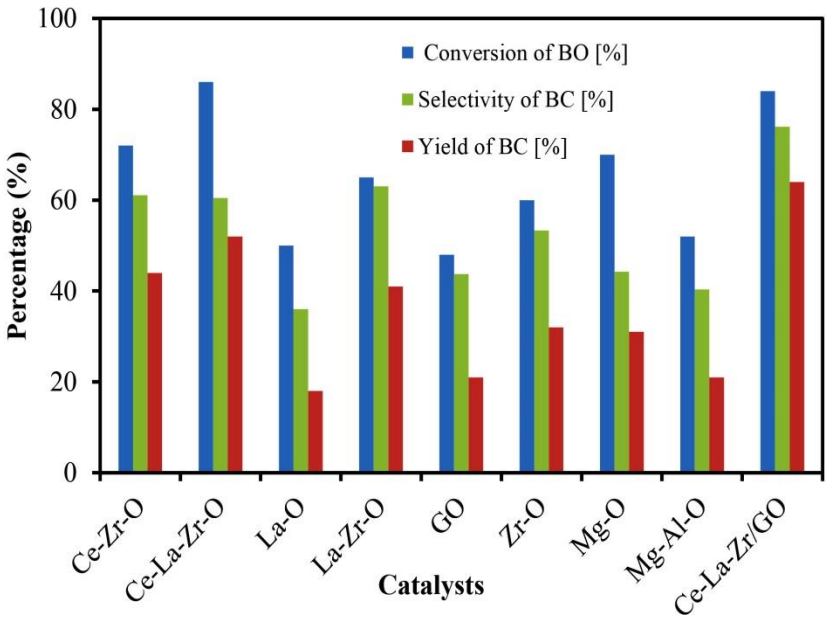

Figure 8: Effect of different metal oxide, and mixed metal oxide heterogeneous catalysts as well as prepared GO via Hummer's method and Ce-La-Zr/GO inorganic nanocomposite via CHFS on conversion of BO against yield and selectivity of BC. Experimental conditions: Catalyst - Ce-La-Zr/GO; Catalyst loading - 10% (w/w); CO_2 pressure - 75 bar; Reaction temperature – 408 K; Reaction time; 20 h; Stirring speed – 300 rpm.

3.5 Effect of Catalyst Loading

The influence of different catalysts loading (w/w) ranging from 5% - 15% have been studied for the synthesis of BC *via* cycloaddition reaction of CO_2 to BO as shown in Figure 9. It has been observed that with an increase in catalyst loading (w/w) from 5% to 10%, BO conversion was increased from 48% to 84%, and the yield of BC increased from 18% to 64% (see Figure 9). However, with an increase in catalyst loading (w/w) from 10% to 12.5%, there were no significant changes in the conversion of BO and yield of BC, although the separation of the product becomes difficult as the catalyst loading goes beyond 10% (w/w). Furthermore, there were no significant changes in the responses as the catalyst loading exceeded 10% (w/w), except for 15% (w/w) catalyst loading where it was observed that there was a slight drop in the yield of BC. This shows that the active sites required for the reaction of BO and CO_2 to produce BC were sufficient at 10% (w/w) catalyst loading when taking the experimental error of ±2% into consideration. Therefore, based on this study, it can be concluded that at fixed reaction conditions at 408 K, 75 bar and 20 h, 10% (w/w) catalyst loading is the optimum amount of catalyst needed for this reaction.

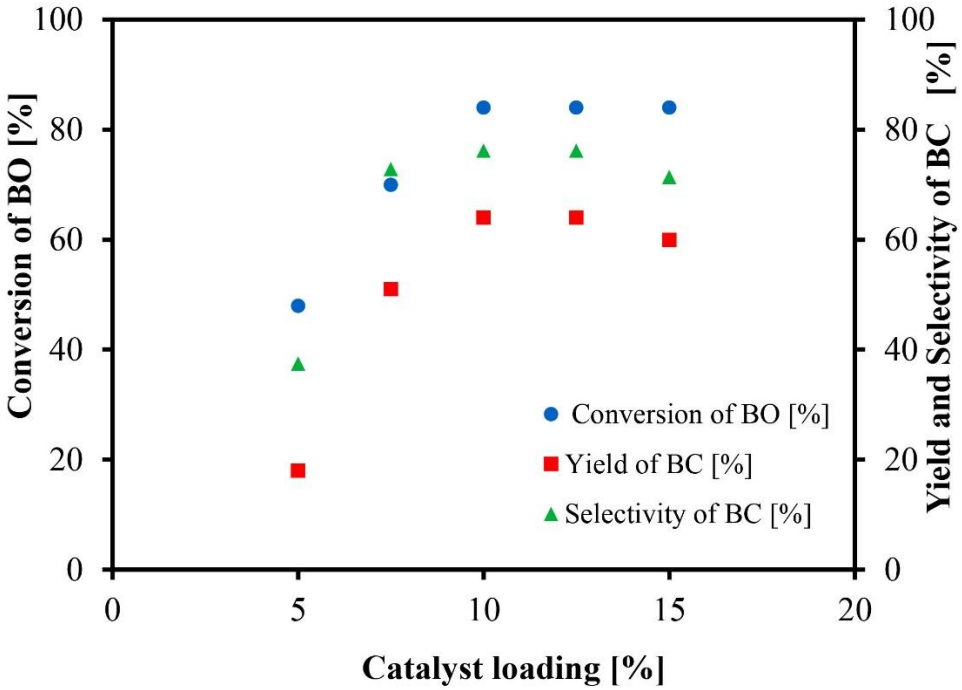

Figure 9: Effect of catalyst loading on conversion of BO against yield and selectivity of BC. Experimental conditions: Catalyst - Ce-La-Zr/GO; Catalyst loading - 10% (w/w); CO_2 pressure - 75 bar; Reaction temperature; 408 K; Reaction time; 20 h, Stirring speed – 300 rpm.

3.6 Effect of Reaction Time

Several experiments were carried out using different reaction time ranging from 16 h to 24 h with a target to conclude the importance of reaction time on the synthesis of BC. The different reaction time of 16 h, 20 h and 24 h at constant reaction conditions of 408 K, 75 bar and 10% catalyst loading for Ce-La-Zr/GO were investigated. Figure 10 shows that the reaction time affects both BO conversion and BC yield significantly. It increases both responses (i.e. BO conversion and BC yield) from the range between 16 and 20 h, while beyond 20 h the conversion of BO and yield of BC remains unchanged, which were 84% and 64% respectively. In contrast, at the reaction time of 16 h, the conversion of BO was 71% and BC yield was 64% while at the reaction time of 20 h, it increases to 80% and 64% respectively. In this study, it is evident that optimum reaction time is 20 h under otherwise identical reaction conditions.

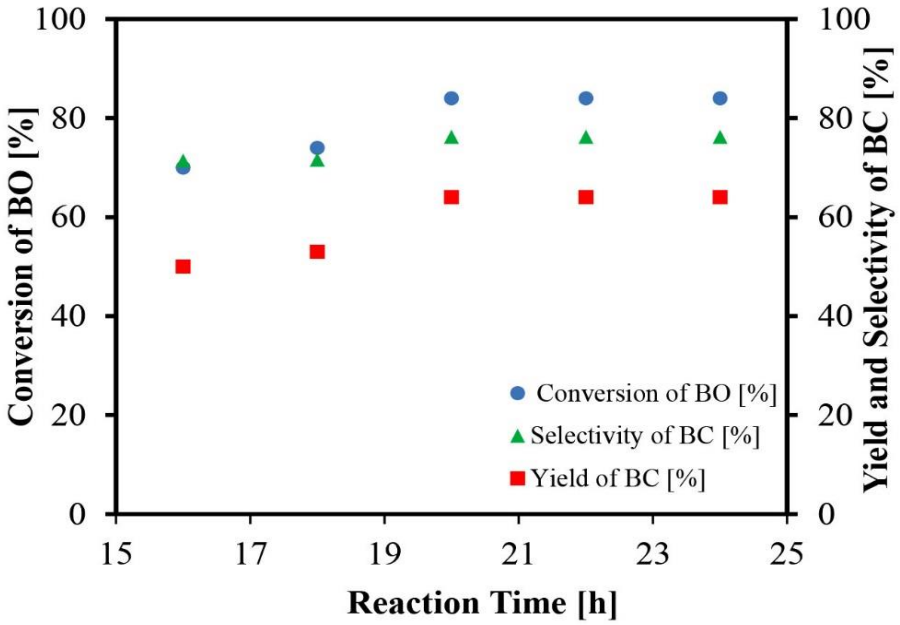

Figure 10: Effect of reaction time on conversion of BO against yield and selectivity of BC. Experimental conditions: Catalyst - Ce-La-Zr/GO; Catalyst loading - 10% (w/w); CO_2 pressure - 75 bar; Reaction temperature; 408 K; Stirring speed – 300 rpm

3.7 Effect of Reaction Temperature

In this study, the synthesis of BC through the reaction of BO and CO_2 were carried out at a different reaction temperature from 368 K to 408 K in order to establish the effect of reaction temperature on BO conversion, BC yield and selectivity. The reaction conditions for this study were set at 10% (w/w) catalyst loading, the CO_2 pressure of 75 bar for 20 h. As it was expected, the higher the temperature, the more the conversion of BO into carbonates isomers and oligomers. Figure 11 shows the temperature dependence on the yield and selectivity of BC.

It was observed from Figure 11 that there was a corresponding increase in conversion of BO, BC yield and selectivity as temperature increases from 368 K to 408 K, however, further increase of temperature from 408 K to 430 K, there was a significant drop of BC yield from 64% to 58%. The selectivity drops from 76% to 64% whilst its BO conversion increases from 84% to 90%. These results are in good agreement with similar work published by Adeleye et al [11]. Based on this study, 408 K was found to be the optimum reaction temperature for synthesis of BC.

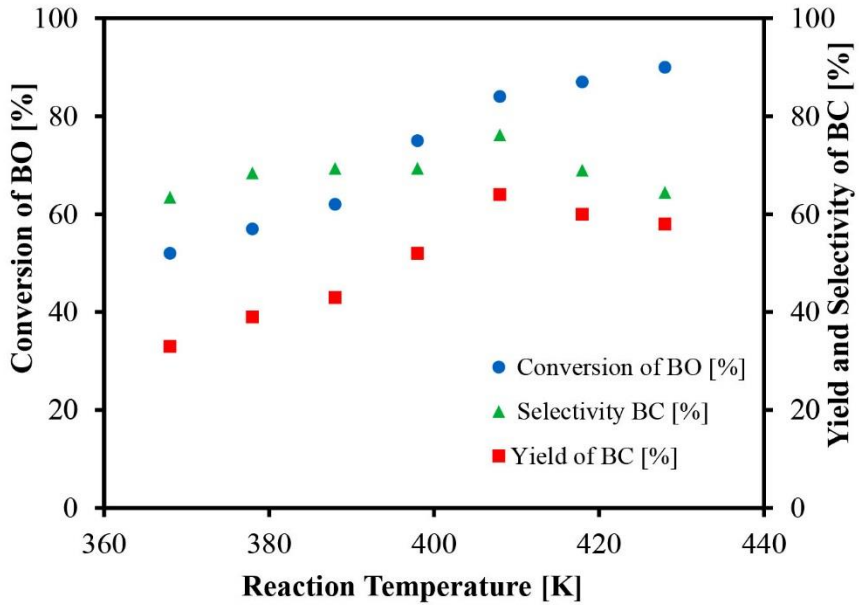

Figure 11: Effect of reaction temperature on conversion of BO against yield and selectivity of BC. Experimental conditions: Catalyst - Ce-La-Zr/GO; Catalyst loading - 10% (w/w); CO_2 pressure - 75 bar; Reaction time; 20 h; Stirring speed – 300 rpm.

3.8 Effect of CO_2 Pressure

The application of CO_2 pressure is very significant for the synthesis of BC through the reaction of BO and CO_2. It has been reported that application of CO_2 in the supercritical state can influence reaction system positively and improve the mass transfer efficiency of the reactants, thereby, creating a shift in the reaction equilibrium which tends to open up the thermodynamic limitation of the reaction [49,50]. The effect of CO_2 pressure on BO conversion and BC yield were investigated to determine the optimum CO_2 pressure for the cycloaddition reaction of CO_2 to BO. These experimental studies were carried out in a high-pressure reactor at 408 K with CO_2 pressure ranging from 55 bar to 105 bar for 20 h and the obtained experimental results were shown in Figure 12. It can be seen in Figure 12 that an increase in CO_2 pressure from 55 bar to 75 bar increases the BO conversion and the BC yield. As a result, selectivity increased rapidly from 58% to 76%, however, beyond 75 bar there were further increase in BO conversion but the yield of BC dropped slightly. This can be explained by the pressure effect on the concentrations of CO_2 and epoxide in the reaction [51]. Furthermore, the drop in yield could also be attributed to the form of by-products such as oligomers and isomers which were below the detection limit of GC-FID used in the analysis and therefore yields of the by-products were not calculated. Based on the experimental results of the investigation, it can be concluded that the optimum CO_2 pressure for this reaction is 75 bar. This study shows the supercritical

condition of CO_2, there is an improvement in polarity and solubility of BO conversion as the reaction pressure increases.

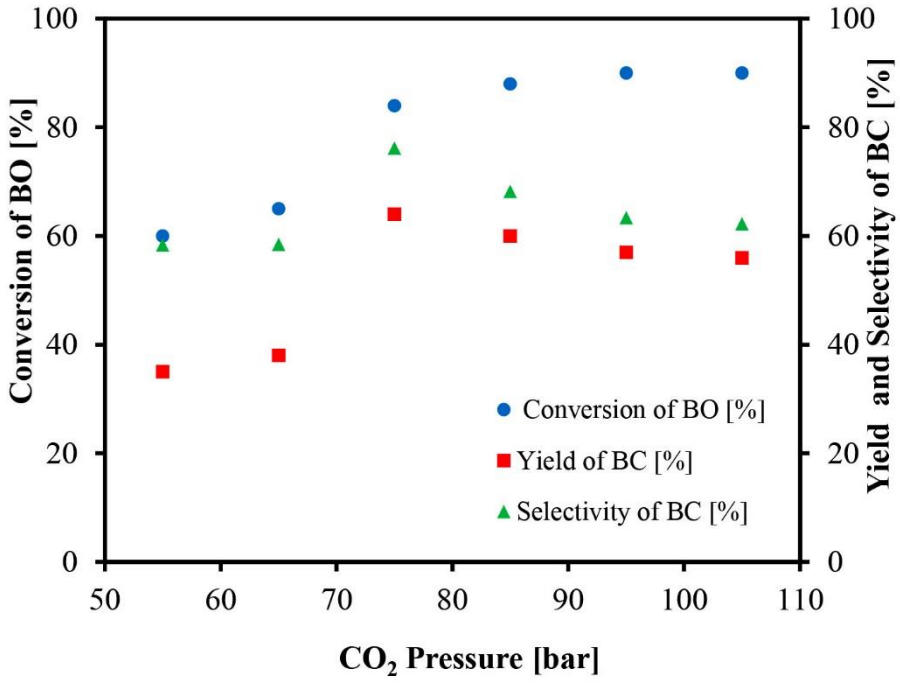

Figure 12: Effect of reaction CO_2 pressure on conversion of BO against yield and selectivity of BC. Experimental conditions: Catalyst - Ce-La-Zr/GO; Catalyst loading - 10% (w/w); Reaction temperature – 408 K; Reaction time; 20 h; Stirring speed – 300 rpm.

3.9 Catalyst reusability studies

One of the vital characteristics of an industrial catalyst is the ability to regenerate without losing its catalytic activity and also providing resistance to deactivation. The heterogeneous catalyst reusability experiments were conducted to investigate the catalytic activity of the best performed heterogeneous catalyst. Ceria-lanthana-zirconia/graphene nanocomposite reusability test was investigated in different runs. The experiments were carried out in a high-pressure reactor at optimum reaction conditions of temperature 408 K, the CO_2 pressure of 75 bar, fresh 10% (w/w) catalyst loading of Ce-La-Zr/GO for 20 h. The first used catalyst was recovered by filtration from the reaction mixture and washed with acetone, which was dried in an oven for 12 h at 323 K. The catalyst was later reused for 5 different runs subjected to the same reaction conditions and as it can be observed in Figure 13 that the conversion of BO, yield and selectivity of BC were approximately the same with an experimental error of ±2%. It can be concluded that Ce-La-Zr/GO catalyst still maintains its catalytic activity after several runs.

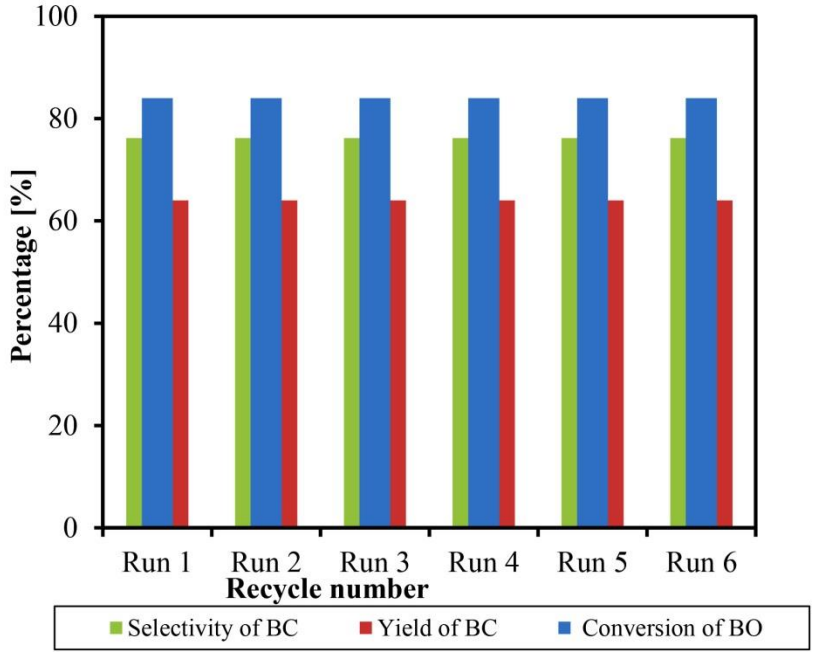

Figure 13: Catalyst reusability studies on conversion of BO against yield and selectivity of BC. Experimental conditions: Catalyst - Ce-La-Zr/GO; Catalyst loading - 10% (w/w); Reaction temperature – 408 K; Reaction time; 20 h; Stirring speed – 300 rpm

4. CONCLUSIONS

This study showcases the transformation of CO_2 to a value-added chemical (e.g. BC) using a highly active heterogeneous catalyst instead of other means of CO_2 emissions reduction such as CCS which is not economically viable when compared with utilisation. The synthesis of BC through cycloaddition reaction of CO_2 and BO has been successfully carried out using a high-pressure reactor in the presence of various heterogeneous catalysts without any solvent. It was observed that the supercritical state of CO_2 influences reaction system positively and improves the mass transfer efficiency of the reactants. The experimental results revealed that among the used heterogeneous catalysts ceria-lanthana-zirconia/graphene oxide (Ce-La-Zr/GO) catalyst was found to be the best-performed catalyst and the optimum reaction condition was found at 408 K, 75 bar CO_2 pressure, 10% (w/w) catalyst loading and 20 h reaction. Ce-La-Zr/GO catalyst was easily recycled and reused several times without any reduction in its catalytic performance.

Acknowledgments

The authors are thankful to Magnesium Elektron Limited (MEL) Chemicals Ltd, UK for supplying some of the catalysts for this work. V. N. Onyenkeadi would like to acknowledge London South Bank University (LSBU) and PATIB venture for supporting this research.

5. REFERENCES

[1] Metz B, Intergovernmental Panel on Climate Change. Working Group III. IPCC special report on carbon dioxide capture and storage. Cambridge University Press for the Intergovernmental Panel on Climate Change; 2005.

[2] Sakakura T, Kohno K. The synthesis of organic carbonates from carbon dioxide. Chem Commun 2009:1312. doi:10.1039/b819997c.

[3] Aresta M, Dibenedetto A. Industrial utilization of carbon dioxide (CO2). Dev. Innov. Carbon Dioxide Capture Storage Technol., vol. 2, Elsevier; 2010, p. 377–410. doi:10.1533/9781845699581.4.377.

[4] North M, Pasquale R, Young C. Synthesis of cyclic carbonates from epoxides and CO2. Green Chem 2010;12:1514. doi:10.1039/c0gc00065e.

[5] Olabi AG. Renewable energy and energy storage systems. Energy 2017;136:1–6. doi:10.1016/j.energy.2017.07.054.

[6] Badea CDNSC-CCA. CO2 capture from syngas generated by a biomass gasification powerplant with chemical absorption process.pdf. Energy 2018;149:925–36.

[7] Mobley PD, Peters JE, Akunuri N, Hlebak J, Gupta V, Zheng Q, et al. Utilization of CO2 for ethylene oxide. Energy Procedia 2017;114:7154–61. doi:10.1016/j.egypro.2017.03.1878.

[8] Fujita S, Arai M. Chemical fixation of carbon dioxide: Synthesis of cyclic carbonate, dimethyl carbonate, cyclic urea and cyclic urethane. J Japan Pet Inst 2005;48:67–75. doi:10.1627/jpi.48.67.

[9] Wei R-J, Zhang X-H, Du B-Y, Fan Z-Q, Qi G-R. Selective production of poly(carbonate–co–ether) over cyclic carbonate for epichlorohydrin and CO2 copolymerization via heterogeneous catalysis of Zn–Co (III) double metal cyanide complex. Polymer (Guildf) 2013;54:6357–62. doi:10.1016/j.polymer.2013.09.040.

[10] North M, Pasquale R. Mechanism of Cyclic Carbonate synthesis from epoxides and CO_2. Angew Chemie Int Ed 2009;48:2946–8. doi:10.1002/anie.200805451.

[11] Adeleye AI, Patel D, Niyogi D, Saha B. Efficient and greener synthesis of propylene carbonate from carbon dioxide and propylene oxide. Ind Eng Chem Res 2014;53:18647–57. doi:10.1021/ie500345z.

[12] Meylan FD, Moreau V, Erkman S. CO2 utilization in the perspective of industrial ecology, an overview. J CO2 Util 2015;12:101–8. doi:10.1016/j.jcou.2015.05.003.

[13] Aresta M, Michele. My journey in the CO_2-chemistry wonderland. Coord Chem Rev

2017;334:150–83. doi:10.1016/j.ccr.2016.06.004.

[14] Alves M, Grignard B, Mereau R, Jerome C, Tassaing T, Detrembleur C. Organocatalyzed coupling of carbon dioxide with epoxides for the synthesis of cyclic carbonates: catalyst design and mechanistic studies. Catal Sci Technol 2017;7:2651–84. doi:10.1039/C7CY00438A.

[15] Aresta M, Dibenedetto A. Carbon dioxide as building block for the synthesis of organic carbonates. J Mol Catal A Chem 2002;182–183:399–409. doi:10.1016/S1381-1169(01)00514-3.

[16] He Q, O'Brien JW, Kitselman KA, Tompkins LE, Curtis GCT, Kerton FM. Synthesis of cyclic carbonates from CO_2 and epoxides using ionic liquids and related catalysts including choline chloride–metal halide mixtures. Catal Sci Technol 2014;4:1513–28. doi:10.1039/C3CY00998J.

[17] Goyal M, Nagahata R, Sugiyama J, Asai M, Ueda M, Takeuchi K. Direct synthesis of diphenyl carbonate by oxidative carbonylation of phenol using Pd–Cu based redox catalyst system. J Mol Catal A Chem 1999;137:147–54. doi:10.1016/S1381-1169(98)00122-8.

[18] Marchegiani M, Nodari M, Tansini F, Massera C, Mancuso R, Gabriele B, et al. Urea derivatives from carbon dioxide and amines by guanidine catalysis: Easy access to imidazolidin-2-ones under solvent-free conditions. J CO2 Util 2017;21:553–61. doi:10.1016/j.jcou.2017.08.017.

[19] Adeleye AI, Kellici S, Heil T, Morgan D, Vickers M, Saha B. Greener synthesis of propylene carbonate using graphene-inorganic nanocomposite catalysts. Catal Today 2015;256:347–57. doi:10.1016/j.cattod.2014.12.032.

[20] Dai W, Yang W, Zhang Y, Wang D, Luo X, Tu X. Novel isothiouronium ionic liquid as efficient catalysts for the synthesis of cyclic carbonates from CO_2 and epoxides. J CO_2 Util 2017;17:256–62. doi:10.1016/j.jcou.2016.12.010.

[21] Morales G, Delgado X, Galeano LA. Effect of the halogen ligand in [Mn(salen)X] complexes on the catalytic styrene epoxidation in scCO2. J CO_2 Util 2015;12:82–5. doi:10.1016/j.jcou.2015.06.002.

[22] Song B, Guo L, Zhang R, Zhao X, Gan H, Chen C, et al. The polymeric quaternary ammonium salt supported on silica gel as catalyst for the efficient synthesis of cyclic carbonate. J CO2 Util 2014;6:62–8. doi:10.1016/j.jcou.2014.03.005.

[23] Shaikh A-AG, Sivaram S. Organic Carbonates. Chem Rev 1996;96:951–76. doi:10.1021/cr950067i.

[24] Saada R, Kellici S, Heil T, Morgan D, Saha B. Greener synthesis of dimethyl carbonate using a novel ceria-zirconia oxide/graphene nanocomposite catalyst. Appl Catal B Environ 2015;168–169:353–62. doi:10.1016/j.apcatb.2014.12.013.

[25] Fujita S-I, Arai M, Bhanage BM. Transformation and utilization of carbon dioxide to value-added products over heterogeneous catalysts. Transform. Util. Carbon Dioxide, 2014, p. 39–53. doi:10.1007/978-3-642-44988-8_2.

[26] Xu J, Xu M, Wu J, Wu H, Zhang W-H, Li Y-X. Graphene oxide immobilized with ionic liquids: facile preparation and efficient catalysis for solvent-free cycloaddition of CO_2 to propylene carbonate. RSC Adv 2015;5:72361–8. doi:10.1039/C5RA13533H.

[27] Dai WL, Luo SL, Yin SF, Au CT. The direct transformation of carbon dioxide to organic carbonates over heterogeneous catalysts. Appl Catal A Gen 2009;366:2–12. doi:10.1016/j.apcata.2009.06.045.

[28] Saada R, AboElazayem O, Kellici S, Heil T, Morgan D, Lampronti GI, et al. Greener synthesis of dimethyl carbonate using a novel tin-zirconia/graphene nanocomposite catalyst. Appl Catal B Environ 2018;226:451–62. doi:10.1016/j.apcatb.2017.12.081.

[29] Huang CH, Tan CS. A review: CO_2 utilization. Aerosol Air Qual Res 2014;14:480–99. doi:10.4209/aaqr.2013.10.0326.

[30] Kellici S, Acord J, Ball J, Reehal HS, Morgan D, Saha B. A single rapid route for the synthesis of reduced graphene oxide with antibacterial activities. RSC Adv 2014;4:14858. doi:10.1039/c3ra47573e.

[31] Wang S, Han S, Xin G, Lin J, Wei R, Lian J, et al. High-quality graphene directly grown on Cu nanoparticles for Cu-graphene nanocomposites. Mater Des 2018;139:181–7. doi:10.1016/j.matdes.2017.11.010.

[32] Nair RR, Blake P, Grigorenko AN, Novoselov KS, Booth TJ, Stauber T, et al. Fine structure constant defines visual transparency of graphene. Science 2008;320:1308. doi:10.1126/science.1156965.

[33] Zhang Z, Brown S, Goodall JBM, Weng X, Thompson K, Gong K, et al. Direct continuous hydrothermal synthesis of high surface area nanosized titania. J Alloys Compd 2009;476:451–6. doi:10.1016/j.jallcom.2008.09.036.

[34] Hummers WS, Offeman RE. Preparation of graphitic oxide. J Am Chem Soc 1958;80:1339–1339. doi:10.1021/ja01539a017.

[35] Chaudhry AA, Haque S, Kellici S, Boldrin P, Rehman I, Khalid FA, et al. Instant nano-hydroxyapatite: a continuous and rapid hydrothermal synthesis. Chem Commun 2006;0:2286. doi:10.1039/b518102j.

[36] Kellici S, Gong K, Lin T, Brown S, Clark RJH, Vickers M, et al. High-throughput continuous hydrothermal flow synthesis of Zn-Ce oxides: unprecedented solubility of Zn in the nanoparticle fluorite lattice. Philos Trans R Soc A Math Phys Eng Sci 2010;368:4331–49. doi:10.1098/rsta.2010.0135.

[37] Yan X, Cui X, Li LS. Synthesis of large, stable colloidal graphene quantum dots with tunable size. J Am Chem Soc 2010;132:5944–5. doi:10.1021/ja1009376.

[38] Lester E, Blood P, Denyer J, Giddings D, Azzopardi B, Poliakoff M. Reaction engineering: The supercritical water hydrothermal synthesis of nano-particles. J Supercrit Fluids 2006;37:209–14. doi:10.1016/j.supflu.2005.08.011.

[39] Cabañas A, Li J, Blood P, Chudoba T, Lojkowski W, Poliakoff M, et al. Synthesis of nanoparticulate yttrium aluminum garnet in supercritical water–ethanol mixtures. J Supercrit Fluids 2007;40:284–92. doi:10.1016/j.supflu.2006.06.006.

[40] Appaturi JN, Adam F. A facile and efficient synthesis of styrene carbonate via cycloaddition of CO2 to styrene oxide over ordered mesoporous MCM-41-Imi/Br catalyst. Appl Catal B Environ 2013;136–137:150–9. doi:10.1016/j.apcatb.2013.01.049.

[41] Srivastava R, Srinivas D, Ratnasamy P. Syntheses of polycarbonate and polyurethane precursors utilizing CO2 over highly efficient, solid as-synthesized MCM-41 catalyst. Tetrahedron Lett 2006;47:4213–7. doi:10.1016/j.tetlet.2006.04.057.

[42] Kellici S, Acord J, Power NP, Morgan DJ, Coppo P, Heil T, et al. Rapid synthesis of graphene quantum dots using a continuous hydrothermal flow synthesis approach. RSC Adv 2017;7:14716–20. doi:10.1039/C7RA00127D.

[43] Bêche E, Charvin P, Perarnau D, Abanades S, Flamant G. Ce 3d XPS investigation of cerium oxides and mixed cerium oxide (Ce xTiyOz). Surf. Interface Anal., vol. 40, 2008, p. 264–7. doi:10.1002/sia.2686.

[44] Klaewkla R, Arend M, Hoelderich WF. A Review of Mass Transfer Controlling the Reaction Rate in Heterogeneous Catalytic Systems. Mass Transf - Adv Asp 2011:667–84. doi:10.5772/22962.

[45] Szent-gyorgyi A. Diffusion and Reaction. Elem Chem React Eng 2006:813.

[46] Dou J, Sun Z, Opalade AA, Wang N, Fu W, Tao F (Feng). Operando chemistry of catalyst surfaces during catalysis. Chem Soc Rev 2017;46:2001–27. doi:10.1039/C6CS00931J.

[47] Clerici MG, Kholdeeva OA. Liquid phase oxidation via heterogeneous catalysis: organic synthesis and industrial applications. Hoboken, New Jersey: John Wiley & Sons, Inc.;

2013. doi:10.1002/9781118356760.

[48] Patel D, Saha B. Heterogeneous kinetics and residue curve map (RCM) determination for synthesis of *n*-hexyl acetate using ion-exchange resins as catalysts. Ind Eng Chem Res 2007;46:3157–69. doi:10.1021/ie060725x.

[49] Zou G, Jiang H-F, Chen M-C. Chemical reactions in supercritical carbon dioxide. ChemInform 2004;35:191–8. doi:10.1002/chin.200429261.

[50] Baiker A. Supercritical fluids in heterogeneous catalysis. Chem Rev 1999;99:453–74. doi:10.1021/cr970090z.

[51] Xiong Y, Bai F, Cui Z, Guo N, Wang R. Cycloaddition reaction of carbon dioxide to epoxides catalyzed by polymer-supported quaternary phosphonium salts. J Chem 2013:9. doi:10.1155/2013/261378.